

Folded Floating-Gate CMOS Biosensor for the Detection of Charged Biochemical Molecules

Baozhen Chen, Archana Parashar, and Santosh Pandey

Abstract—A folded floating-gate CMOS biosensor is realized for the detection of charged biochemical molecules. The biosensor comprises a field-effect transistor with a floating-gate, a control-gate, and a sensing area. Charged biochemical molecules placed on the sensing area induce a voltage on the floating-gate and a relative shift in the threshold characteristics. Compared to conventional devices, the floating-gate here is folded to span the entire device. This allows us to place the sensing area above the field-effect transistor (FET), thus reducing the total device area. The fabricated devices show good sensitivity to the polarity and concentration of charged poly amino acids. Possible applications of the device include electronic detection of spatial and temporal charge migration such as in biological processes.

Index Terms—Bio-FET, CMOS sensor, electronic charge sensing, floating gate transistor.

I. INTRODUCTION

IN RECENT YEARS, there has been significant advances in the area of noninvasive, portable sensors that would couple chemical, and biological entities with semiconductor devices and integrated circuits [1]–[5]. These include electronic sensors for the detection of chemicals, DNA hybridization, enzyme reactions, action potentials, and protein complexes. To address the issues of postprocessing, label-free detection, and bulky instrumentation in traditional electrochemical sensors [2]–[6], a CMOS-compatible extended floating-gate field-effect transistor (EGFET) device have been demonstrated for the electronic detection of electrolytes [7] and DNA hybridization [8], [9]. In these EGFETs, the floating-gate is capacitively coupled to the sensing area (where biochemical species are adsorbed) in one direction and to the control-gate (where the readout voltage is applied) in the other direction [7]–[9]. The threshold voltage is a function of the applied control-gate voltage and the charge on the sensing area. Fluctuations in the amount of biochemical charge are electronically detected by a corresponding shift in the threshold voltage. However, in the present EGFETs, the floating-gate topology is bifurcated and spans in two directions [7], [8], which increases the overall device area. In addition, the sensing area of the device is large ($40\ \mu\text{m} \times 40\ \mu\text{m}$ to $100\ \mu\text{m} \times 100\ \mu\text{m}$) [8] and is placed far from the FET in order

Manuscript received December 21, 2010; revised April 22, 2011; accepted April 25, 2011. Date of publication May 02, 2011; date of current version October 26, 2011. This work is supported by a NSF-CMMI-1000808 grant from the National Science Foundation. The associate editor coordinating the review of this paper and approving it for publication was Dr. Dwight Woolard.

The authors are with the Department of Electrical and Computer Engineering, Iowa State University, Ames, IA 50014 USA (e-mail: chen.baozhen@gmail.com; archana@iastate.edu; pandey@iastate.edu).

Color versions of one or more of the figures in this paper are available online at <http://ieeexplore.ieee.org>.

Digital Object Identifier 10.1109/JSEN.2011.2149514

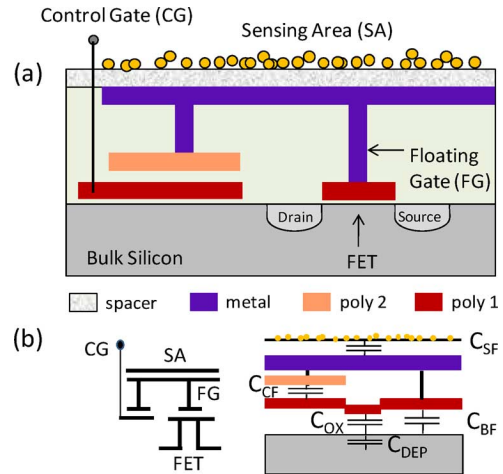


Fig. 1. (a) Structure of the proposed bio-FET showing its floating-gate, control-gate, and sensing area. (b) Equivalent capacitive model for the device.

to isolate the test species from the transistor [7]–[9]. As a solution, nonplanar EGFETs have been proposed to shrink the sensing area by combining microelectromechanical systems (MEMS) micromachining and CMOS fabrication steps [4].

Here, we present an extended floating-gate biosensor with a folded floating-gate topology (Fig. 1). The device comprises a FET with a control-gate, a floating-gate, and a sensing area. The basic working principle is similar to previous EGFET designs [7]–[9]. However, the floating-gate here is placed above the control-gate and is folded to cover the entire device (Fig. 1). This allows us to utilize the top device area as the sensing area which is now directly above the FET. Thus, the sensing and detection is done at the same location on the chip. The device is fully CMOS-compatible and its charge sensitivity is comparable to other EGFET devices [7]–[9].

II. METHODOLOGY

The induced voltage V_{FG} on the floating-gate of the biosensor device shown in Fig. 1 is written as [7]–[9]

$$V_{FG} = \frac{C_{CF}}{C_T} V_{CG} + \frac{C_{GS}}{C_T} V_{SB} + \frac{C_{GD}}{C_T} V_{DS} + \frac{Q_{F0} - Q_i}{C_T} \quad (1)$$

$$C_T = C_{CF} + C_{SF} + C_{BF} + C_{GS} + C_{GD} + C_{OX} // C_{DEP} \quad (2)$$

where C_{CF} represents capacitance between control-gate and floating-gate, C_{SF} is the capacitance between sensing area and floating-gate, C_{BF} is the capacitance between floating-gate and the bulk, C_T is the total capacitance of the device, V_{CG} is the applied voltage on the control-gate, Q_{F0} is the static charge on

floating-gate, and Q_i is the total induced charge on sensing area. The other device parameters used in (1) and (2) are the oxide capacitance C_{OX} , floating-gate to source capacitance C_{GS} , floating-gate to drain capacitance C_{GD} , and the FET depletion capacitance C_{DEP} . The effective threshold voltage V_T is related to the original threshold voltage V_{T0} (i.e., with no solution on the sensing area) and can be modulated by charges on top of the sensing area as shown in (3) and (4). Assuming there is minimal change in the applied voltages (V_{DS} and V_{SB}) and the amount of static charge Q_{F0} , the effective change in threshold voltage ΔV_T is proportional to the amount of fluctuation in the surface charge on the sensing area ΔQ_i

$$V_T = V_{T0} - \frac{C_{GS}}{C_T} V_{SB} - \frac{C_{GD}}{C_T} V_{DS} - \frac{Q_{F0} - Q_i}{C_T} \quad (3)$$

$$\Delta V_T = V_T - V_{T(DI_water)} = -\frac{\Delta Q_i}{C_T}. \quad (4)$$

In our experiments, Q_{F0} is taken as the reference charge on the floating-gate with deionized (DI) water on the sensing area. When the charged biomolecules are brought close to the surface of the sensing area, they induce countercharges (i.e., Q_i) in the floating-gate [1]. This alters the induced voltage on the floating-gate and shifts the effective threshold voltage. Positively charged molecules increase V_{FG} and thus a smaller V_{CG} is required to turn on the device. This produces a lower threshold voltage (V_T) and a negative shift in the current-voltage (I - V) curve compared to that for DI water. Alternatively, negatively charged molecules lower the floating-gate voltage V_{FG} and require a higher control-gate voltage V_{CG} to turn on the device. This is measured by a higher threshold voltage and a positive shift in the I - V curve compared to that for DI water.

The biosensor devices are designed in standard CMOS AMI Semiconductor (AMIS) 1.5 μm library. After a series of design optimization steps, the sensing area is conservatively chosen as $14.4 \mu\text{m} \times 28.4 \mu\text{m}$. The smallest possible device area can be further scaled as $13\lambda \times 14\lambda$, where 2λ is the minimum FET gate length or half of the technology node ($\lambda = 0.8$ in our case). The W/L ratio is 3:1. The thicknesses of the gate oxide and interpoly oxide are approximately 31 and 60 nm, respectively. A 1 μm thick SiO_2 spacer separates the floating-gate and the charged molecules on the sensing area. Next, a 3-D model is built in Synopsys Sentaurus Structure Device Editor adopting the design topology and dimensions [Fig. 2(a)]. In each simulation, a fixed amount of electronic charge is placed on the sensing area [Fig. 2(b)]. The simulation results indicate that the floating-gate voltage V_{FG} increases linearly with the control-gate voltage V_{CG} . Furthermore, for a fixed V_{CG} , increasing the charge density linearly increases the amount of voltage induced on the floating-gate similar to [9]. From our simulations, 1×10^3 electrons/ μm^2 of charge on the sensing area produces a 0.95 V change in the floating-gate voltage V_{FG} . As shown in (4), decreasing the sensing area does not necessarily improve the device sensitivity as both C_{SF} and ΔQ_i are reduced. For comparison purposes, the reported EGFETs have a sensitivity of 5.44 V/C (i.e., one electron charge per μm^2 produces 14 μV voltage shift) [9].

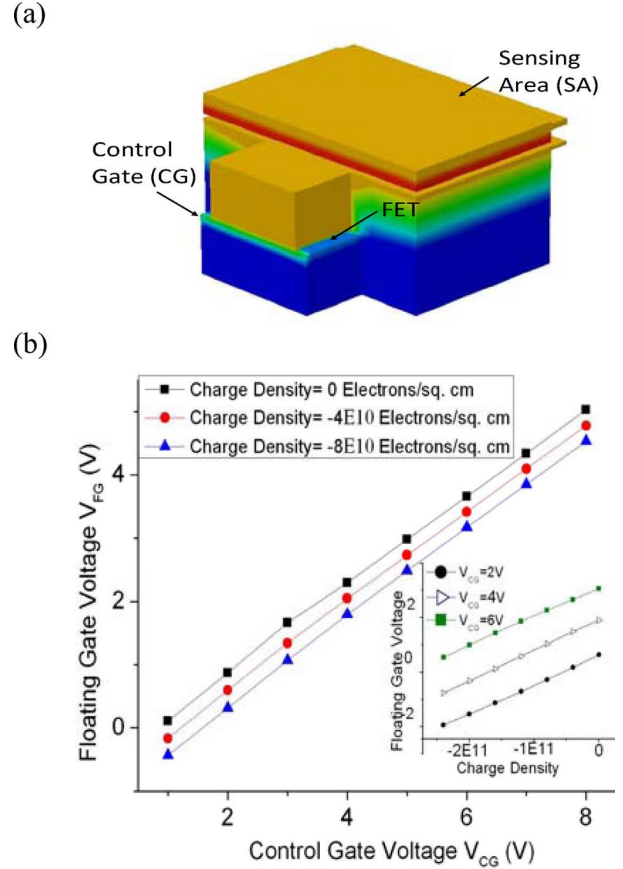


Fig. 2. (a) Three-dimensional device structure created using Sentaurus Structure Device Editor. (b) A graph of the floating-gate voltage versus the applied control-gate voltage at three fixed charge densities on the sensing area (SA). The inset shows the variation of the floating-gate voltage with charge density on the sensing area (SA) at three fixed control-gate voltages.

The layout is fabricated in CMOS AMIS 1.5 μm process and packaged in 40-pin dual in-line package (DIP). Each chip comprises individual devices of varying areas ($14.4 \mu\text{m} \times 28.4 \mu\text{m}$ to $100 \mu\text{m} \times 100 \mu\text{m}$). The packaged chips are tested using a HP4145 semiconductor parameter analyzer. Unlike conventional ChemFETs [2], no postprocessing or additional coating is needed. The sensing area is physically isolated from the floating-gate by overlay glass (1 μm thick) deposited during the last step of CMOS fabrication. A polydimethylsiloxane (PDMS) layer with a 1.5×1.5 mm opening is placed on the chip for protection of the contact pads and bonding wires. A certain volume (0.8–1.2 μL) of a previously prepared solution of biochemical molecules is dropped on the fabricated chip. A custom LabView program is used to apply the voltage V_{CG} on the control-gate. The series (5–10) of I - V curves are recorded and compared with that for DI water (used as reference). To refresh the device or to test another biomolecular concentration, the chip's surface is first rinsed (3–5 times) and then tested with DI water to obtain the reference I - V curve. The new solution is subsequently dropped on the chip surface and the I - V characteristics are recorded.

The following charged biochemicals are used for testing the devices: poly-L-lysine (0.01%), poly-L-histidine (0.01%), poly glutamic acid (0.5%), poly aspartic acid (PAA) (0.5%), poly

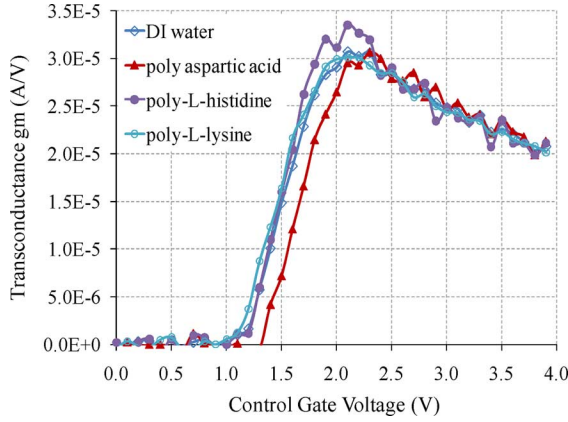


Fig. 3. Transconductance versus control-gate voltage are plotted for poly amino acids and compared with the DI water reference curve.

styrenesulfonic acid sodium salt (PSASS), and poly diallyl dimethyl ammonium chloride (PDDAC).

III. RESULTS AND DISCUSSION

Fig. 3 plots the measured transconductance (g_m) versus control-gate voltage V_{CG} for different charged poly amino acids on the sensing area of the biosensor device. The drain voltage is fixed at 0.4 V and the control-gate voltage is swept from 0 to 4 V. Each curve is an average of 10–12 experimental runs. The g_m curve with DI water is similar to the measured response under dry conditions. Compared to the DI water reference, the g_m curves for poly-L-histidine and poly-L-lysine are shifted to the left. This is because both poly amino acids, being positively charged, produce an increase in the floating-gate voltage and a decrease in the threshold voltage. Negatively charged poly aspartic acid and poly glutamic acid shift the $g_m - V_{CG}$ curves to right of DI water reference.

The threshold voltages are extracted from Fig. 3 using the transconductance method [7]. For the case of DI water reference, the threshold voltage is 1.5 V. A differential threshold voltage ($\Delta V_T = V_{T_poly} - V_{T_DI}$) is calculated as the difference between the threshold voltages of a device under test and that for DI water. For positively charged poly-L-histidine and poly-L-lysine, the ΔV_T values are -0.1 and -0.08 V, respectively. The ΔV_T values for negatively charged poly aspartic acid and poly glutamic acid are 0.35 V and 1.2 V respectively. Both poly-L-histidine and poly-L-lysine have a much lower (0.01% w/v) concentration which explains their smaller ΔV_T magnitude. Poly aspartic acid and poly glutamic acid are at a higher (0.5% w/v) concentration and hence produce a larger ΔV_T magnitude. Each I–V measurement is done 5–8 times and repeated (5–8 times) again after refreshing the device using the above mentioned steps (Section II). The ΔV_T values are consistent which indicates reliability in detecting biochemical charges using the bio-FETs.

We also measure the subthreshold characteristics of the biosensor devices. The drain voltage is fixed at 2.5 V and the control-gate voltage is swept from 0 V to 2 V. The subthreshold I–V curves are recorded for different concentrations of PAA solution (Fig. 4). The devices are refreshed after each run of

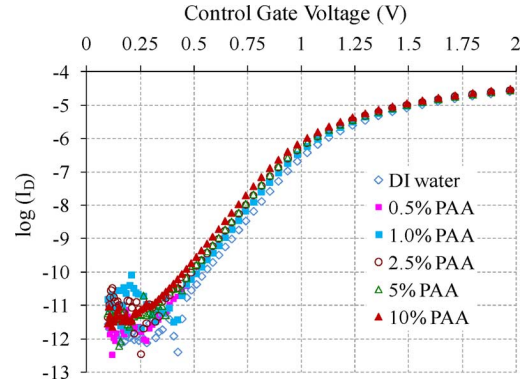


Fig. 4. Subthreshold current versus drain voltage is plotted for different PAA concentrations and compared with the DI water reference curve.

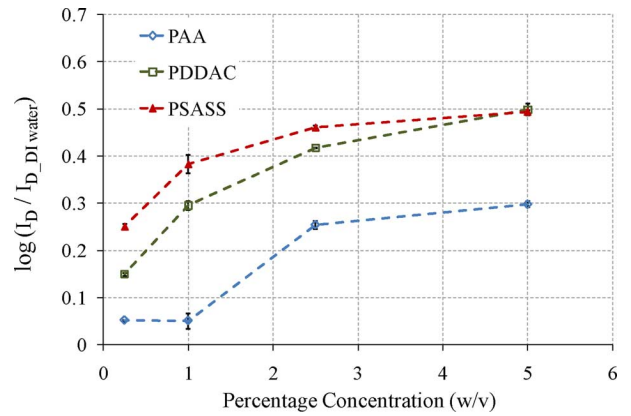


Fig. 5. Relative shift in the logarithmic drain current (difference in a device's drain current with poly amino acid and with DI water) versus percentage concentration of four poly amino acids (PAA, PDDAC, PSASS).

5–8 trials and reused. The subthreshold I–V curves show a consistent shift to the left with increasing PAA concentration.

A higher concentration of PAA molecules increases the surface potential and lowers the threshold voltage V_T . The subthreshold slope S is unaltered, indicating that the charge distribution is undisturbed during individual experiments [7]. These results are also expected from our simulations.

To show concentration-dependent change in the threshold voltage, two other poly amino acids (PSASS and PDDAC) are tested (Fig. 5). Similar to the PAA case in Fig. 4, subthreshold I–V curves are measured for different concentrations of the poly amino acids. The relative shifts in the logarithmic subthreshold I–V curve from that for DI water are plotted in Fig. 5. Error bars are included for each data point. In all the three cases, we observe a small current shift at lower ($< 1\%$ w/v) charge concentrations. As the charge concentration increases, the current shift increases and eventually approaches saturation at around 5% w/v concentration. The saturation point corresponds to the scenario where all the surface sites are occupied with charged molecules. The standard deviation in each data point is small ($< 8\%$) which indicates consistency and reliability of the measurements.

The folded floating-gate device topology can be useful for detecting spatial charge variations within a biological specimen. Since the sensing area is directly above the FET, each device can

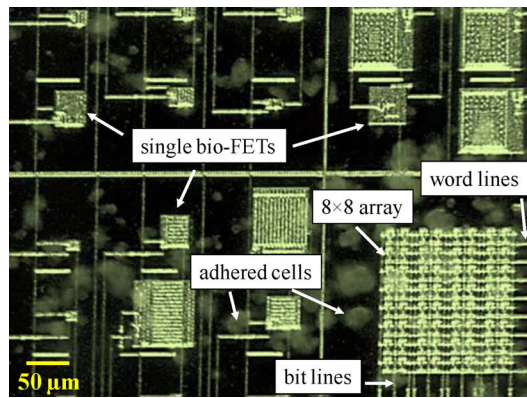


Fig. 6. Snapshot of the fabricated chip showing single and an array of biosensor devices. Cell lines placed on the chip adhered to the surface and are growing into neurons (translucent globules).

be viewed as a pixel for charge sensing. Several devices in an array can then be viewed as an electronic pixel array that can be read in parallel. It is worth mentioning here that such an array implementation would be challenging with earlier EGFETs as their floating-gate is bifurcated and the large sensing areas are placed far away from the FETs.

To show initial feasibility of the biosensor devices for VLSI applications and biological detection, we fabricated an 8×8 array of the proposed devices ($14.4 \mu\text{m} \times 28.4 \mu\text{m}$) (Fig. 6). Bit and word lines are included for parallel readout of multiple devices in the array [6]. The control-gates of a single row are connected to form a bit line while drain electrodes of a single column are connected to form a word line. Each of the 8 bit and word lines is addressable by an external analog-digital converter and a custom LabView program. A device with simultaneously activated bit and word lines is automatically read and its I-V characteristics are recorded. We observe that the individual biosensor devices in the array behave electrically similar to the isolated devices (Figs. 3–5). Fabrication in a smaller technology node (possibly $0.18 \mu\text{m}$ or 40 nm) can further scale the array dimensions.

As a “proof-of-concept” for on-chip cell growth and viability, neuronal cell lines (suspended in standard cell culture media) are dropped on the fabricated chip which then adhered to the chip surface and grew over time (Fig. 6). The on-chip cell culture is monitored for three days. The snapshot in Fig. 6 shows successful adherence and growth of neurons on the chip surface three days after placing the cell lines. The measured I-V characteristics of the biosensor devices in the array are stable all through the three days of neuronal growth. This indicates good physical and chemical isolation of the floating-gate and minimal penetration of ions in the culture media through the overlay glass.

Floating-gate MOS devices are known to trap residual charges during the CMOS fabrication process, which alter the effective threshold voltage of these devices [10]. Techniques such as UV erasing, Fowler–Nordheim tunneling, and hot electron injection are employed to remove this charge from the floating-gate [10]. Studies have shown that the amount of trapped charge is almost the same in all floating-gate transistors fabricated on the same die and in the same fabrication run [11].

In our experiments, we also did not observe any noticeable changes in threshold voltage among the different devices fabricated on the same die. This may be because our devices are placed close to one another on the same die and fabricated at the same time. Furthermore, since we are measuring the differential threshold voltage (4), the effects of residual charge on our experimental results are expected to be minimal. However, if required, this initial charge can be eliminated by any of the abovementioned techniques used for other floating-gate MOS devices.

IV. CONCLUSION

In conclusion, we presented a folded floating-gate topology for an EGFET where the sensing area is placed directly above the FET. This allows us to shrink the lateral device dimensions compared to the conventional bifurcated floating-gate topology. Our tests suggest good physical and chemical isolation of the floating-gate from the sensing area. The transconductance and subthreshold characteristics provide a reliable means of detecting charge fluctuations on the sensing area of individual devices. The biosensor device is fully CMOS-compatible and is shown feasible for VLSI applications with parallel readout. Biocompatibility and successful growth of neuronal cells on the chip surface has been demonstrated. Such an electronic biosensor can enable possible real-time, noninvasive observation of biologically relevant processes which involve charge migration, or localization including cell growth and regeneration.

REFERENCES

- [1] M. Shinwar, M. Deen, and D. Landheer, “Study of the electrolyte-insulator-semiconductor field-effect transistor (EISFET) with applications in biosensor design,” *Microelectron. Reliab.*, vol. 47, pp. 2025–2057, 2007.
- [2] M. J. Schoning and A. Poghossian, “BioFEDs (Field-effect devices): State-of-the-art and new directions,” *Electroanalysis*, vol. 19, pp. 1893–1900, 2006.
- [3] L. Chen, M. Topinka, B. LeRoy, R. Westervelt, K. Maranowski, and A. Gossard, “Charge-imaging field-effect transistor,” *Appl. Phys. Lett.*, vol. 79, no. 8, 2001.
- [4] D.-S. Kim, J.-E. Park, J.-K. Shin, P. Kim, G. Lim, and S. S. Park, “An extended gate FET-based biosensor integrated with a Si microfluidic channel for detection of protein complexes,” *Sens. Actuators B*, vol. 117, pp. 488–494, 2006.
- [5] S. Meyburg, M. Goryll, J. Moers, S. Ingebrandt, S. Bocker-Meffert, H. Luth, and A. Offenhausser, “N-Channel field-effect transistors with floating gates for extracellular recordings,” *Biosens. Bioelectron.*, vol. 21, pp. 1037–1044, 2006.
- [6] J. M. Rabaey, A. Chandrakasan, and B. Nikolic, *Digital Integrated Circuits*. Upper Saddle River, NJ: Prentice-Hall, 2003.
- [7] N. Shen, Z. Liu, C. Lee, B. Minch, and E. Kan, “Charge-based chemical sensors: A neuromorphic approach with chemoreceptive neuron MOS transistors,” *IEEE Trans. Electron Devices*, vol. 50, no. 10, pp. 2171–2178, Oct. 2003.
- [8] M. Barbaro, A. Bonfiglio, L. Raffo, A. Alessandrini, P. Facci, and I. Barakbarak, “A CMOS, fully integrated sensor for electronics detection of DNA hybridization,” *IEEE Electron Device Lett.*, vol. 27, no. 7, pp. 595–597, Jul. 2006.
- [9] M. Barbaro, A. Bonfiglio, and L. Raffo, “A charge-modulated FET for detection of biomolecular process: Conception, modeling, and simulation,” *IEEE Trans. Electron Devices*, vol. 53, no. 1, pp. 158–166, Jan., 2006.
- [10] T. Tokuda, A. Yamamoto, K. Kagawa, M. Nunoshita, and J. Ohta, “A CMOS image sensor with optical and potential dual imaging function for on-chip bioscientific applications,” *Sens. Actuators A*, vol. 125, pp. 273–280, 2006.

- [11] E. Rodriguez-Villegas, M. Jimenez, and R. Carvajal, "On dealing with the charge trapped in floating gate MOS (FGMOS) transistors," *IEEE Trans. Circuits Syst.-II Express Briefs*, vol. 54, no. 2, pp. 156–160, 2007.

Baozhen Chen received the B.S. degree in condensed matter physics from the University of Science and Technology of China (USTC), Hefei, China, in 2005 and the Ph.D. degree in electrical engineering from Iowa State University, Ames, in 2010, and worked on the design, fabrication, and testing of CMOS-based charge sensors. He also worked on microfluidic assays for high-throughput behavioral analysis of micro-organisms.

He is currently with a semiconductor company in Raleigh, NC.

Archana Parashar received the B.Sc. degree in biochemistry from Patna University, Patna, India, in 2009 and the M.S. degree in biochemistry from the Industrial Toxicology Research Centre (ITRC), India, in 2010. Currently, she is working towards the Ph.D. degree at the Department of Electrical and Computer Engineering, Iowa State University, Ames.

Her current projects include the design and measurement of CMOS-compatible bioelectronics, behavioral microfluidics for *C. elegans*, and high-throughput screening platforms for pathogens.

Santosh Pandey received the B.Tech. degree in electrical engineering from the Indian Institute of Technology, Kharagpur, in 1999 and the Ph.D. degree in electrical engineering from Lehigh University, Lehigh, PA, 2006. His doctoral dissertation was focused on developing an integrated MEMS/CMOS silicon-based platform for performing high-throughput cellular electrophysiology.

In 2006, he joined the Department of Electrical Engineering, Iowa State University, as an Assistant Professor. His research interests lie in engineering high-throughput screening platforms for cell cultures and whole organisms by integrating semiconductors, microfluidics, systems biology, and image-processing processing tools.